Preprints (www.preprints.org) | NOT PEER-REVIEWED | Posted: 1 September 2021 doi:10.20944/preprints202109.0013.v1

Article

Construction of a novel chimeric dextransucrase fused to the carbohydrate-binding module CBM2a

Reinaldo Fraga Vidal [1,*], Roberto C. Arísticas Ribalta [1], Lisandra Martínez Valdés [1], Meinardo Lafargue Gámez [1], Amanda Montes Alvarez [1], Arianne Rubio Sánchez [1], Eric Dubreucq [2], Benoît Moreau [3]

[1] Cuban Research Institute on Sugarcane By-Products (ICIDCA). P.O. Box 4026, 11000, Havana, Cuba. Tel. 053-7-696-7015; Fax: 053-7-988243; reynaldo.fraga@icidca.azcuba.cu
[2] SupAgro Montpellier, 2 Place Viala, 34060 Montpellier Cedex 2, France; Eric.Dubreucq@supagro.fr
[3] Haute Ecole Province de Henaut – Condorcet, Rue Paul Pastur 11, 7800 Ath, Belgium. E. mail: benoit.moreau@condorcet.be
* Correspondence: reynaldo.fraga@icidca.azcuba.cu (R.F.); Tel. 053-7-696-7015

Abstract: The lactic acid bacteria (LAB) have great potential to produce homoexopolysaccharides (HoPS), have been the subject of extensive research efforts, given their health benefits and physicochemical properties. The HoPS functional properties are determined by structural characteristics of varied molecular weights, types of glycosidic linkages, degrees of branching and chemical composition. The dextransucrases (DSases) are responsible of the synthesis of a kind of HoPS (dextran polymers), which are among the first biopolymers produced at industrial scale with applications in medicine and biotechnology. The concept of glycodiversification opens additional applications for DSases. In that sense the design and characterization of new DSases is of prime importance. Previously, we described the isolation and characterization of a novel extracellular dextransucrase (DSR-F) encoding gene. In this study, from DSR-F, we design a novel chimeric dextransucrase DSR-F-ΔSP-ΔGBD-CBM2a, where DSR-F-ΔSP-ΔGBD is fused to the carbohydrate-binding module (CBM2a) of the β-1-4 exoglucanase/xylanase Cex (Xyn10A) of *Cellulomonas fimi* ATCC 484. This dextransucrase variant is active and without alteration in its specificity. The DSR-F-ΔSP-ΔGBD-CBM2a is purified by cellulose affinity chromatography for the very first time. Our results indicate that new hybrids and chimeric DSases with novel binding capacity to cellulose can be designed to obtain glyco-biocatalysts from renewable lignocellulosic materials.

Keywords: dextransucrases; GH70; lactic acid bacteria; sucrose-active enzymes; carbohydrate binding module; glucansucrase; cellulose binding domain; *Leuconostoc*

1. Introduction

Homoexopolysaccharides (HoPS) produced by lactic acid bacteria (LAB) have received great research efforts into their physicochemical and bioactive properties [1]. The individual functional properties of HoPS are determined by their chemical composition, molecular weights, types of glycosidic linkages as well as degree and arrangement of branches [2]. The structural diversity of HoPS is a result of the unmatched variety of possible osidic bonds between sugar monomers, offering an extensive range of functionalities of interest for food, feed, pharmaceuticals, cosmetics and chemicals industries [3-6].

Dextrans are among the first microbial HoPS produced at industrial scale [7]. Microorganisms of the genera *Lactobacillus*, *Streptococcus*, *Weissella*, *Leuconostoc*, *Pediococcus*, *Oenococcus* and *Acetobacter* [8] produce these polysaccharides. The *Leuconostoc mesenteroides* NRRL B-512F is used for the synthesis of the most common and widespread commercial dextran. The biopolymer's main chain contains α(1-6) linked glucosyl residues with only 5% of α(1-3) linked branches [7]. The dextran fractions of controlled molecular weight and their numerous derivatives are mainly used in medicine, pharmaceuticals and fine chem-

© 2021 by the author(s). Distributed under a Creative Commons CC BY license.

Preprints (www.preprints.org) | NOT PEER-REVIEWED | Posted: 1 September 2021 doi:10.20944/preprints202109.0013.v1

istry [9,10]. The extracellular glucansucrase (dextransucrase) DSR-S, a 6-α-D-glucosyltransferase (EC 2.4.1.5) is responsible for the polymer production [11]. This enzyme belongs to the glycoside hydrolase family 70 (GH70) according to the CAZy classification (http://www.cazy.org/) [12]. The GH70 family consists of a large and diverse group of polymerases and branching enzymes, some of them being mainly active on sucrose and others on starch substrates [13,14].

The catalytic domain of GH70 presents the typical $(\alpha/\beta)_8$ barrel of glucansucrases, the three amino acids (D551, E589, D662, DSR-S numbering) forming the catalytic triad are highly conserved in the GH70 family [15-17].

The study of GH70 enzymes with different specificities from new LAB strains and from mining genome data sets could provide new insights in structure-function relationships of glucansucrases as well as enlarge the natural dextransucrase repertoire available for industrial application [18]. The Cuban Research Institute on Sugarcane By-products (ICIDCA) has a collection of LAB strains isolated from sugarcane and sugarcane derivatives. Some of them have already been characterized to some extent [19-21]. In the present study, a chimeric dextransucrase fused to the carbohydrate-binding module (CBM2a) of the exoglucanase/xylanase Cex (Xyn10A) of *Cellulomonas fimi* ATCC 484 was obtained. This variant, fully active, was purified by cellulose affinity chromatography and partially characterized.

2. Results and Discussion

2.1. Design of a Chimeric Dextransucrase (DSR-F-ΔSP-ΔGBD-CBM2a) Fused to the Carbohydrate Binding Module CBM2a

Based on the 3D structural model of DSR-F-ΔSP-ΔGBD (Fig. 1B), a chimeric dextransucrase fused to the carbohydrate binding module CBM2a (DSR-F-ΔSP-ΔGBD-CBM2a) was constructed (Fig. 1A and 1C). Deleting the two APY repeat units from the C-terminal end of DSR-F and adding the CBM2a, allowed further investigation of this domain fusion on the specificity of the chimeric fused variant.

Preprints (www.preprints.org) | NOT PEER-REVIEWED | Posted: 1 September 2021 doi:10.20944/preprints202109.0013.v1

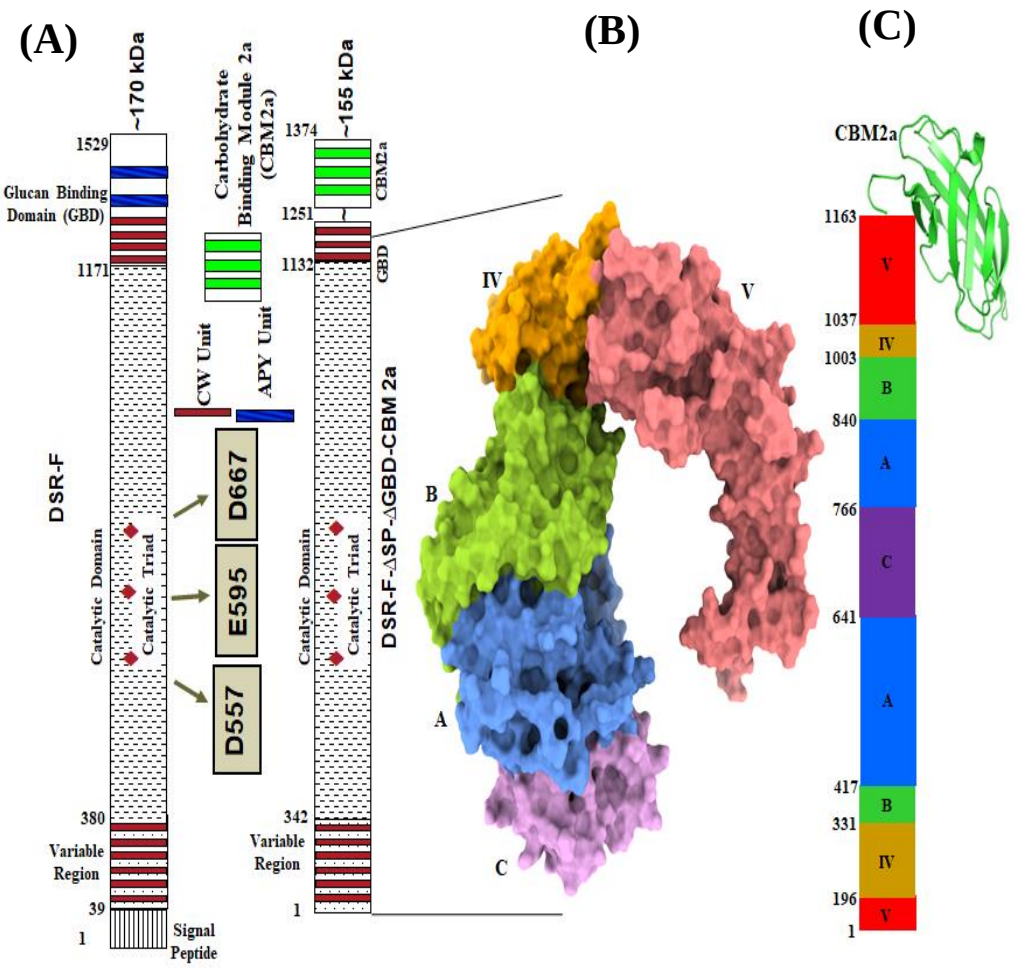

Figure 1. (A). Primary structure representation of the dextransucrase DSR-F of *Leuconostoc citreum* B/110-1-2 and its truncated variant DSRF-ΔSP-ΔGBD. **(B)**. 3D structure model of DSRF-ΔSP-ΔGBD, five different domains are highlighted, in red (domain V), yellow (domain IV), green (domain B), blue (domain A), and magenta (domain C) **(C)**. Linear schematic representation of DSRF-ΔSP-ΔGBD domain organization with CBM2a fused to the C-terminal end.

The recombinant DSR-F enzyme was previously produced without part of its C-terminal glucan binding domain (Fig. 1A, DSR-F-ΔSP-ΔGBD). This deletion of the C-terminal domain V including a cell wall (CW) repeat and the two APY repeats did not affect the DSR-F-ΔSP-ΔGBD specificity and efficiency [19]. Other examples of APY repeats that have been deleted without adverse effect on other GH70 and related enzymes have been observed in alternansucrase, inulosucrase, and branching sucrase BSR-B [22-24].

2.2. Subcloning of DSR-F-ΔSP-ΔGBD to Obtain DSR-F-ΔSP-ΔGBD-CBM2a in the Expression Vector pdsrF-CBM2a. Purification of the Fusion Protein DSR-F-ΔSP-ΔGBD-CBM2a

The construction of plasmid pdsrF-CBM2a allows the inducible expression of DsrF-ΔSP-ΔGBD fused in its carboxyl end region with the carbohydrate binding module CBM2a of Cex, a β-1,4-exo-glucanase of *Cellulomonas fimi* ATCC 484. The fusion of the CBM2a to a dextransucrase is reported for the very first time. The presence of the CBM2a module seems to not affect the ability to form dextran polymer by the fusion enzyme DsrF-ΔSP-ΔGBD-CBM2a (Fig. 2_A and B), and it will permit its purification for further characterization and future immobilization on cellulosic or lignocellulosic materials. A success-

Preprints (www.preprints.org) | NOT PEER-REVIEWED | Posted: 1 September 2021 doi:10.20944/preprints202109.0013.v1

ful dextransucrase fusion for immobilization is the case of DSR-S from *Leuconostoc mesenteroides* B-512FMC to glutathione S-transferase (GST), resulting in a novel and completely active fused truncated variant [25].

The purification of DsrF-ΔSP-ΔGBD-CBM2a from the soluble fraction of the *E. coli* DH10B (pdsrF-CBM2a) was performed using regenerated amorphous cellulose (RAC) as an affinity matrix. The purified protein migrated as a single band with an apparent molecular mass of 155 kDa and a 90-95% purity estimated by densitometry (Fig. 2_B). This is the first report of the use of a cellulose-based matrix for the purification of a dextransucrase by affinity chromatography. The levels of purified protein are greater than those achieved by the immobilized metal ion affinity chromatography (IMAC) (data not shown). This may be because RAC has a higher binding capacity (365 mg of protein per gram of RAC) than any other commercial resin used to purify proteins (10-40 mg of proteins per gram of resin) [26].

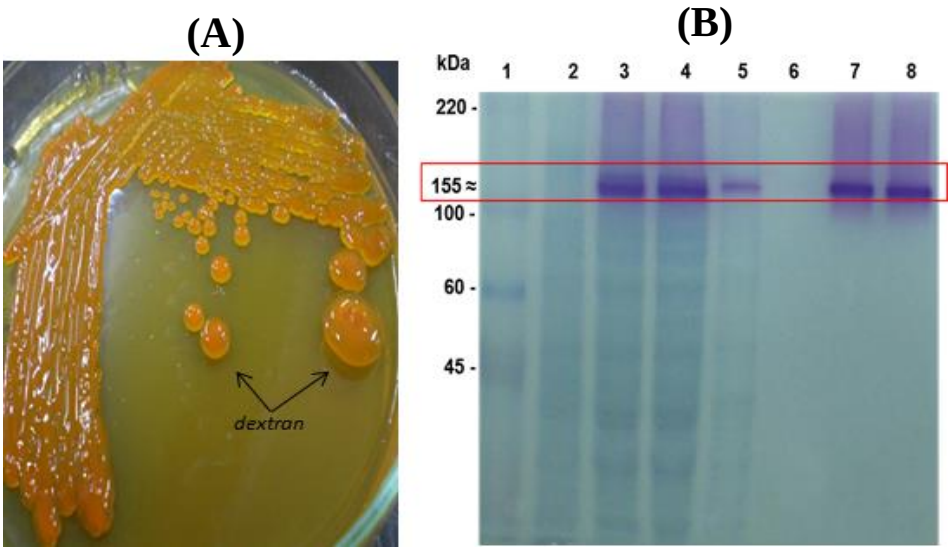

Figure 2. Production of DsrF-ΔSP-ΔGBD-CBM2a in *E. coli* DH10B. **(A)** Detection of dextransucrase activity through the formation of dextran on LBT agar plate. **(B)** SDS-PAGE of DsrF-ΔSP-ΔGBD-CBM2a purification, stained combining two detection methods. Zymography of the proteins with dextransucrase activity (colored bands), followed by detection of total proteins by negative staining with imidazole and zinc sulfate salts (transparent bands). The formation of the dextran polymer demonstrates the activity of the fusion. (1) Molecular Weight Marker (ColorBurst™, Sigma-Aldrich Co.). (2) Soluble fraction of *E. coli* DH10B (pSE380) cell lysate as negative control. (3) Soluble fraction of *E. coli* DH10B (pdsrF-CBD) cell lysate. (4) Flowthrough fraction, not retained by the RAC. (5) Fraction of the 1st washed of column (8 Column Volumes, CV). (6) - Fraction of the 2nd washed of column (12 CV). (7 and 8) - Fractions eluted.

2.3. Action of DSR-F-ΔSP-ΔGBD-CBM2a in Polymerization and Acceptor Reactions

A polymerization reaction with sucrose was carried out to ensure the chimeric DSR-F-ΔSP-ΔGBD-CBM2a behave in the same way as the DSR-F-ΔSP-ΔGBD variant. As dextransucrase GTF180 from *Lb. reuteri* 180 [27] and alternansucrase (ASR) from *L. citreum* NRRL B-1355 [28], DSR-F-ΔSP-ΔGBD-CBM2a and DSR-F-ΔSP-ΔGBD are also striking examples of α-transglucosylases among GH70 glucansucrases. They catalyze a bi-modal population of glucan, comprising a high molar mass (HMM, $2x10^7$ g.mol^{-1}) dextran and a low molar mass gluco-oligosaccharides (LMM, DP<8, around 1300 g. mol^{-1}) from sucrose, as estimated by size exclusion chromatography (Fig. 3-I). This result corroborates the dextran formation observed in Fig. 2A and 2B. In addition, it suggests a semi-processive elon-

Preprints (www.preprints.org) | NOT PEER-REVIEWED | Posted: 1 September 2021 doi:10.20944/preprints202109.0013.v1

gation mechanism, as for other GH70 enzymes, where smaller oligosaccharides are produced in a non-processive mode at the beginning of a reaction. When a critical length is reached a processive mechanism starts helped by glucan-binding domains [29].

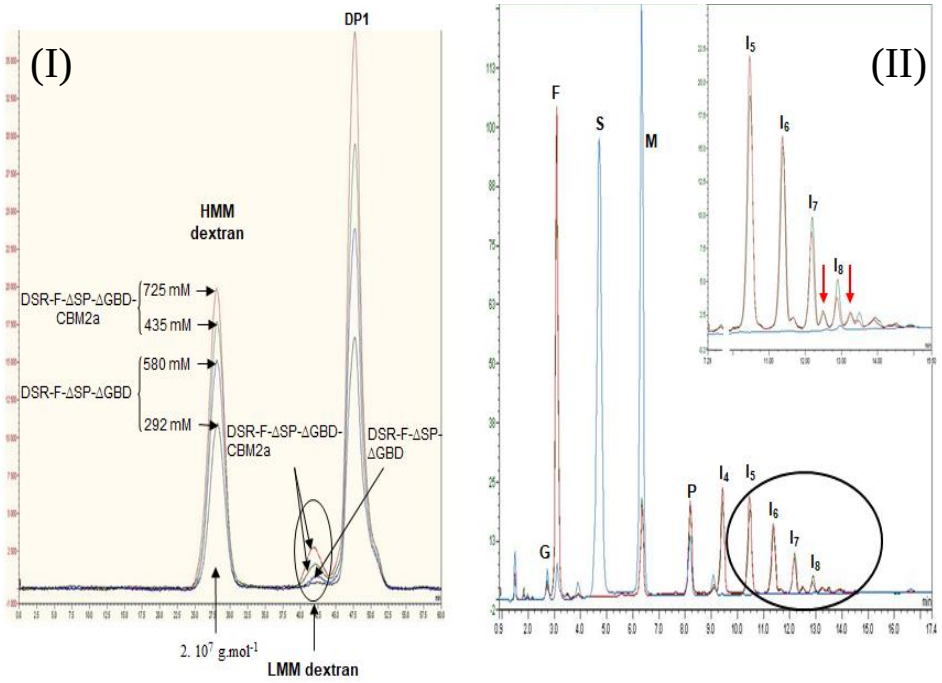

Figure 3. **(I)**-Analysis of HPSEC chromatograms synthesized using the chimeric dextransucrase DSR-F-ΔSP-ΔGBD-CBM2a (from sucrose 580 mM and 725 mM) and DSR-F-ΔSP-ΔGBD (from sucrose 292 mM and 435 mM) with 50 mM sodium acetate buffer, pH 5.5 and 1 U.mL^{-1} of enzyme. Enzymatic reactions were stopped after 24 h. Peak identification: **HMM dextran** high molecular mass dextran (2.10^7 g.mol^{-1} as estimated by HPSEC-MALLS), **LMM dextran** low molecular mass dextran (oligosaccharides of DP<8), **DP1** Fructose. **(II)**-Analysis of HPAEC-PAD chromatograms products synthesized using DSR-F-ΔSP-ΔGBD-CBM2a and DSR-F-ΔSP-ΔGBD from sucrose (292 mM) and maltose (146 mM) with 50 mM sodium acetate buffer, pH 5.5 and 1 U.mL^{-1} of enzyme. Enzymatic reactions were stopped after 24 h. Arrows indicate two extra peaks immediately after the products with degrees of polymerization (DP) of 7 and 8. Peak identification: **G** Glucose, **F** Fructose, **S** Sucrose, **M** Maltose, **P** Panose (DP3), **I4-I8** isomaltooligosaccharides of DP4–DP8. The line with the highest signal of **S** and **M** and no detection of isomaltooligosaccharides corresponds to the enzymatic reaction at the initial time (t = 0 min).

In the acceptor reaction (maltose as acceptor molecule) performed with DSR-F-ΔSP-ΔGBD-CBM2a, a series of analog isomaltodextrins very similar to the ones produced by the recombinant dextransucrase DSR-F-ΔSP-ΔGBD from *L. citreum* B/110-1-2 (Fig. 3-II) were synthesized. The isomalto-oligosaccharides (IMOs) products with 7 and 8 glucose units show two extra peaks (Fig. 3-II, arrows) indicating they were decorated at least with a branched α(1-4) glucose unit. These IMOs products correspond to previously characterized oligodextrans [20]. From these observations, it seems that the cellulose binding domain of DSR-F-ΔSP-ΔGBD-CBM2a does not affect the synthesis of HMM and LMM glucans from sucrose and IMOs products from sucrose/maltose, respectively.

2.4. Action of DSR-F-ΔSP-ΔGBD-CBM2a from Sucrose and Linear Oligodextrans (1500 and 6000 g.mol^{-1})

A reaction using sucrose (292 mM) and 1500 g.mol^{-1} dextran (66.6 mM), a linear α(1-6) glucan with a mean degree of polymerization of 9, was performed. Analyses of the

Preprints (www.preprints.org) | NOT PEER-REVIEWED | Posted: 1 September 2021 doi:10.20944/preprints202109.0013.v1

reaction products showed that a low amount of leucrose could be detected due to the action of fructose as an acceptor (Fig. 4-I). This kind of transglycosylation has been reported to be favored at the start of the dextransucrase reactions [29, 30]. It has been recently suggested that leucrose serves as the substrate for further dextran formation or elongation of IMOs [31]. The IMOs from DP8 to DP12 were glucosyl decorated in the same way by the chimeric dextransucrase DSR-F-ΔSP-ΔGBD-CBM2a and DSR-F-ΔSP-ΔGBD, leading to formation of products clearly observable on HPAEC-PAD chromatograms (Fig. 4-I, arrows). Such chromatographic patterns resulting from the acceptor reaction (oligodextrans as acceptor molecules) is reported for the first time for a DSR-F variant enzyme. According to the specificity of both analyzed enzymes, these modified IMOs could be products being glucosylated to some extent and probably α(1-4) branched glucose units. As a specific population of IMOs seems to act as acceptor molecules to be branched, two factors could be involved with this observation. Structural analyses of dextrans have identified a relation between the degree of branching and the rms radii of the polymers where a comparatively higher proportion of more branched and more compact dextran molecules is increasingly formed. On the other hand branching may also depend on the steric properties of the glucosyl-donor in the active site of the enzyme [31]. However, the structure of these products (DP8-DP12) must be elucidated in more detail.

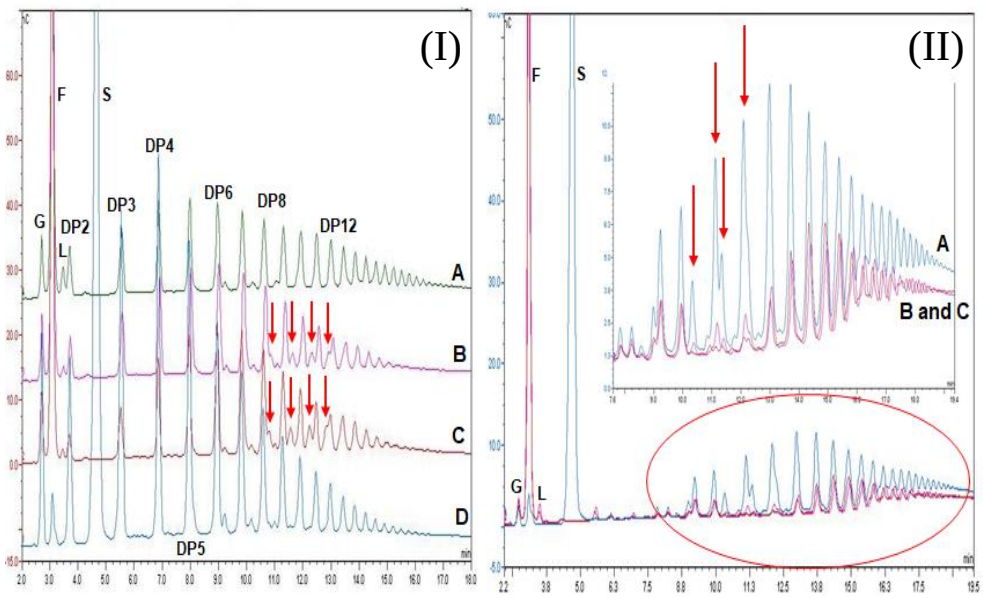

Figure 4. **(I)**- Analysis of HPAEC-PAD chromatograms products synthesized using the chimeric dextransucrase DSR-F-ΔSP-ΔGBD-CBM2a, DSR-F-ΔSP-ΔGBD and native dextransucrase DSR-S from *Leuconostoc mesenteroides* NRRL B-512F from sucrose (292 mM) and dextran 1500 g.mol^{-1} (66.6 mM) with 50 mM sodium acetate buffer, pH 5.5 and 1 U.mL^{-1} of enzyme. Enzymatic reactions were stopped after 24 h, nC, nanocoulombs. **I-(A)**- Enzymatic reaction using DSR-S from *L. mesenteroides* NRRL–B512; **I-(B)**- Enzymatic reaction using DSR-F-ΔSP-ΔGBD recombinant; **I-(C)**- Enzymatic reaction using chimeric dextransucrase DSR-F-ΔSP-ΔGBD-CBM2a; **I-(D)**- Enzymatic reaction using chimeric dextransucrase DSR-F-ΔSP-ΔGBD-CBM2a at the initial time (t = 0 min). Arrows indicate four extra peaks immediately after the products with degrees of polymerization (DP) of 8-12, respectively. **(II)**-Analysis of HPAEC-PAD chromatogram products synthesized using the chimeric dextransucrase DSR-F-ΔSP-ΔGBD-CBM2a and DSR-F-ΔSP-ΔGBD sucrose (292 mM) and dextran 6000 g.mol^{-1} (66.6 mM) with 50 mM sodium acetate buffer, pH 5.5 and 1 U.mL^{-1} of enzyme. Enzymatic reactions were stopped after 24 h. **II-(A)**- Enzymatic reaction using chimeric dextransucrase DSR-F-ΔSP-ΔGBD-CBM2a at the initial time (t = 0 min); **II-(B)**- and **II-(C)**- Enzymatic reaction using DSR-F-ΔSP-ΔGBD-CBM2a and DSR-F-ΔSP-ΔGBD, respectively. Arrows indicate peaks corresponding to modified dextrans from

Preprints (www.preprints.org) | NOT PEER-REVIEWED | Posted: 1 September 2021 doi:10.20944/preprints202109.0013.v1

the initial reaction time. Peak identification: **G** Glucose, **F** Fructose, **L** Leucrose, **S** Sucrose, **DP2-DP12** Isomaltooligosaccharides with a degree of polymerization (DP) from 2 to 12.

A reaction using sucrose (292 mM) and 6000 g.mol^{-1} dextran (66.6 mM), a linear α(1-6) glucan or oligodextran with a mean degree of polymerization of 37 was performed. As seen on HPAEC-PAD chromatograms, the product profile after 24 hours of reaction was different from the initial reaction profile. As in the previous reaction, a low amount of leucrose was also detected. Analyses of the final reaction products showed the intensity of several peaks corresponding to isomaltooligosaccharides decreased, suggesting those products were modified in a similar way by both enzymes DSR-F-ΔSP-ΔGBD-CBM2a and DSR-F-ΔSP-ΔGBD (Fig. 4-II, arrows). So far, only a few studies reported disproportionation reactions of glucansucrases [32,33] which were already studied in detail in other polymerizing enzymes such as levansucrases and inulosucrases [34]. Previous modification of linear α(1-6) short dextrans have only been reported on branching sucrases [13,24]. Therefore, further studies are needed to corroborate a potential utilization of short IMOs as glucosyl donors during dextran synthesis and dextran modifications by dextransucrase-*α*-transglucosylases enzymes.

From the products analysis of the reactions performed in this study, it seems that on dextransucrase DSR-F variants some kind of interactions with IMOs are taking place. Recently, the first functional surface binding site (SBS-A1) for a GH70 family enzyme was described, it binds isomaltose, isomaltotriose, isomaltononaose, panose and oligoalternan [35]. An alignment sequence of SBS-A1 and the equivalent residues in dextransucrase DSR-F is shown in Fig. 5. Several residues are very conserved in both sequences which could be associated with a similar functionality in DSR-F.

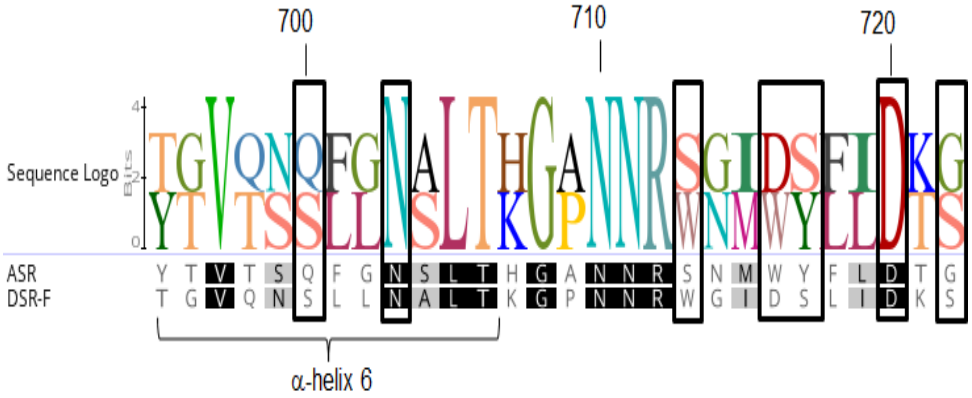

Figure 5. Surface binding site (SBS-A1) sequence comparison. Alignment of the residues corresponding to SBS-A1 of alternansucrase ASR (in black boxes) from *L. citreum* NRRL B-1355 (numbered and α-helix 6 according to ASR in complex with isomaltotriose, PDB entry 6SYQ) with the equivalent residues in dextransucrase DSR-F.

Preprints (www.preprints.org) | NOT PEER-REVIEWED | Posted: 1 September 2021 doi:10.20944/preprints202109.0013.v1

3. Materials and Methods

3.1. Bacterial Strains and Culture Media

Escherichia coli DH10B was used for the subcloning steps and for protein expression with the pSE380 vector (Invitrogen, USA). The screening of *E. coli* colonies expressing functional dextransucrase enzymes was done [20]. LBT medium was used instead of Luria-Bertani (LB) medium [11]. The method relies on the addition of the pH indicator bromothymol blue to LBT media, supplemented with 5% sucrose and 1% glycerol as extra carbon sources. *E. coli* was grown and maintained on LB medium supplemented when needed with ampicillin (100 µg mL^{-1}). All strains were stored at -80 °C in 15% glycerol.

3.2. *Subcloning to Express the dsrF-ΔSP-ΔGBD-CBM2a Gene in E. coli*

The 3.7 kb fragment encoding the truncated variant of DsrF (DsrF-ΔSP-ΔGBD) was digested with the restriction enzymes *Nco*I-*Eco*RI from the pSEdsrF plasmid and inserted into the plasmid pET38b (+) (Novagen), also digested with the same restriction enzymes, to create the 9.5 kb pETdsrF plasmid (Km^r) after the ligation of both fragments. The latter contains the truncated variant dsrF-ΔSP-ΔGBD under the inducible promoter PT7lac, fused at the 3' end to the signal peptide of the exo-β-1,4-glucanase Cex from *Cellulomonas fimi* ATCC 484, at the 5' end of the cellulose binding module (CBM2a) of said enzyme, and to the His_8 tag. Likewise, the truncated variant is also fused to the 5'-terminus of the transcription terminator of bacteriophage T7. The strain of *E. coli* DH10B was transformed with the plasmid pETdsrF, which was subsequently purified and digested with the restriction enzymes *Nco*I-*Avr*II releasing the *dsr*F-ΔSP-ΔGBD fused with the CBM2a and the His_8 tag. This fragment was ligated to the equally digested pSE380 plasmid *Nco*I-*Avr*II, giving rise to the 8.4 kb pdsrF-CBM2a plasmid (Ap^r) containing the *dsr*F-ΔSP-ΔGBD-CBM2a fragment under the inducible Ptrc promoter, fused at the end 3' to the terminator of the transcription of *E. coli* rrnBt1-t2. The strain of *E. coli* DH10B was transformed with this plasmid.

Preprints (www.preprints.org) | NOT PEER-REVIEWED | Posted: 1 September 2021 doi:10.20944/preprints202109.0013.v1

Table 1. Plasmids used in this work.

Plasmids	Description	Reference
pET38b(+)	Replicon colE1, vector used for protein production in E. coli, fused to the signal secretion Cex downstream the PT7lac promoter. It harbours the encoding region for the Carbohydrate-Binding Module. (CBM2a) and a His_8 tag, Km^r, size: 5,8 kb.	Novagen
pSE380	Replicon colE1, vector used for protein production in *E. coli* downstream the PTrc promoter, Ap^r, size: 4,4 kb.	Invitrogen
pSEdsrF	pSE380 *Nco*I-*Eco*RI, fused to the 3,7 kb amplicon *Nco*I-*Eco*RI obtained from pGEMdsrF. Harbours the truncated variant DsrF-ΔSP-ΔGBD, Ap^r, size: 8,1 kb	[19]
pETdsrF	pET38b(+) *Nco*I-*Eco*RI, fused to the 3,7 kb (DsrF-ΔSP-ΔGBD) *Nco*I-*Eco*RI from pSEdsrF, Km^r, size: 9,5 kb.	This work
pdsrF-CBM2a	pSE380 *Nco*I-*Avr*II, fused to the 4,2 kb DNA fragment (DsrF-ΔSP-ΔGBD-CBM2a) *Nco*I-*Avr*II from pETdsrF, Ap^r, size: 8,6 kb.	This work

3.3. *Inducible production of DSR-F-ΔSP-ΔGBD-CBM2a in E. coli*

For the production of the recombinant dextransucrase DsrF-ΔSP-ΔGBD-CBM2a, a colony of the recombinant strain of *E. coli* DH10B (pdsrF-CBM2a), was inoculated in 100 mL invaginated flasks with 10 mL of 2xYT medium supplemented with 100 mM Tris/HCl, pH 6.4, 100 $\mu g.mL^{-1}$ ampicillin at 30 °C, and grown overnight at 175 $r.min^{-1}$. The next day the cultures were diluted 1:100 with the same medium, supplemented with ampicillin 200 $\mu g.mL^{-1}$ and grown at 30 °C to an OD(600nm) 0.5 with shaking at 175 $r.min^{-1}$. Isopropyl-1-thio-β-D-galactopyranoside (IPTG) (inducer of the Ptrc promoter) was added at a final concentration of 2.4 $mmol.L^{-1}$ and incubated 12-14 h at 20 °C with shaking at 175 $r.min^{-1}$. The cells were collected by centrifugation (Eppendorf 5804 R centrifuge) at 10,000 x *g* 15 min at 4 °C and resuspended in the rupture buffer [50 $mmol.L^{-1}$ NaAc, pH 5.4, Triton X 100 0.1% (v/v), $CaCl_2$ 0.05 gL^{-1}, cocktail of protease inhibitors (Roche)] up to an OD(600nm) of 80. Cell disruption was performed by ultrasound in a disruptor (MSP, England). The sample (always kept on ice) was exposed to seven cycles of 1 min, at a constant amplitude of 28 microns, with one minute of rest between cycles. The lysate extract was centrifuged (Eppendorf 5804 R centrifuge) at 21 390 x *g* for 40 min, and the soluble and insoluble fraction of each cell extract was recovered. The samples were stored at -20 ºC until they were used in other analyses.

3.4. *Cellulose Affinity Chromatography (CAC)*

The chimeric DSR-F-ΔSP-ΔGBD-CBM2a was purified by cellulose affinity chromatography (CAC). For this, a matrix of regenerated amorphous cellulose (RAC) obtained from Microgranular Cellulose CC31 (Whatman) was used [36]. The soluble fraction of the sonicate extract (10 mL) was mixed by slow agitation with 5 mL of RAC for 2 hours at 4 °C. The enzyme bound to the matrix was recovered by centrifugation (Eppendorf 5804 R) at 3 500 x *g* for 5 min and packed in a 10 mL column (10 cm X 2 cm ∅, Bio-Rad). The protein was eluted with 1 mL of glycerol 99 %.

3.5. *Determination of Enzymatic Activity Dextransucrase*

The enzymatic activity was performed at 30 °C and 40 °C, in 50 $mmol.L^{-1}$ sodium acetate buffer (pH 5.4), 0.05 gL^{-1} $CaCl_2$, 1 gL^{-1} NaN_3, and 100 gL^{-1} sucrose. The saccharolytic

Preprints (www.preprints.org) | NOT PEER-REVIEWED | Posted: 1 September 2021 doi:10.20944/preprints202109.0013.v1

activity was determined by detecting the levels of free reducing sugars with the dinitrosalicylic acid (DNSA) method [37]. One unit of activity was defined as the amount of enzyme that catalyzes the release of 1 µmol.min^{-1} of fructose under the conditions tested. The concentration of proteins was detected according to [38] using BSA as a standard. All determinations were made in triplicate.

3.6. *SDS-PAGE and Zymograms*

Protein electrophoresis under denaturing conditions (SDS-PAGE) was performed with the XCell SureLockTM Mini-Cell system, with NOVEX Tris–Acetate gels of 1.5-mm thickness, NuPAGE® anti-oxidant and NuPAGE®Tris-Acetate SDS Running Buffer (for Tris-Acetate gels) from Invitrogen. The NuPAGE® Sample Reducing Agent (3 ml) and NuPAGE®LDS Sample Buffer (X4) sample buffer (7.5 ml) were mixed with 20 µl of sample and heated at 70 °C for 10 min prior to being loaded onto gels. Samples containing suspended cells were centrifuged at 10,000 x *g* in a micro-centrifuge before being applied to the gels. Approximately 2 mU of enzyme was loaded onto the gels and electrophoresis was carried out for 1 h at 150 V. The gels were then stained for dextransucrase activity *in situ* according to the procedure of [39] in combination with a reversible negative protein staining method [40]. Precision Plus Protein™ All Blue Standard was included in all electrophoresis runs.

3.7. *Production of High Molecular Weight Dextrans, Maltooligosaccharides, and Linear Dextran Modification*

High-molecular-weight dextran synthesis was performed at 40 °C for 24 h, in buffer 20 mmol.L^{-1} NaAc (pH 5.4), $CaCl_2$ 0.05 gL^{-1}, NaN_3 1 gL^{-1}, sucrose 100 gL^{-1} and 1 U.ml^{-1} of enzyme. Malto-oligosaccharides were produced under the same conditions, except maltose 50 gL^{-1} was added to the reaction. Linear dextrans were modified under the same conditions but 66.6 mM of α-1,6 dextrans (1500 g.mol^{-1} and 6000 g.mol^{-1}; Sigma) was added.

3.8. *High Performance Anion-Exchange Chromatography with Pulsed Amperometric Detection (HPAEC-PAD)*

Synthesized oligosaccharides were analyzed by high HPAEC-PAD using a Dionex Carbo-Pack PA100 4x250 mm column at room temperature. A gradient of sodium acetate (from 6 to 300 mmol.L^{-1} in 28 min) was applied in 150 mmol.L^{-1} NaOH at a flow rate of 1 mL.min^{-1}. Detection was performed with an ED40 Doinex module gold electrode and a reference pH Ag/AgCl. Standards used were glucose, fructose, sucrose, panose, leucrose, prepared as 10 mg.mL^{-1} in buffer 20 mmol.L^{-1} NaAc (pH 5.4). The samples were diluted 10 times in water and were filtered through membranes with pores of 0.20 µm (Sartorius) before injection.

3.9. *High-Performance Size Exclusion Chromatography (HPSEC)*

Glucan molecular weight distributions were determined by HPSEC. For dextran analyses, two Shodex OH-Pack SB-805 and SB-802.5 columns were maintained in series, using an eluent containing 0.45 M of NaN_3 and 1% of ethylene glycol at a flow rate of 0.3 ml min-1. Columns and guard columns were maintained at 70 °C, and samples were filtered through a 0.45-µm-pore-size filter (Sartorius) before injection [29]. The reaction was stopped after 24 h by heating 5 min at 95 °C in a boiling water bath. Calibration standards of commercial dextrans of 2.10^6 g.mol^{-1}, 530.103 g.mol^{-1}, 70x10^3 g.mol^{-1}, and 10x10^3 g.mol^{-1} (Sigma-Aldrich) were used.

4. Conclusions

Preprints (www.preprints.org) | NOT PEER-REVIEWED | Posted: 1 September 2021 doi:10.20944/preprints202109.0013.v1

Both enzymes were able to produce HMM and LMM polymers from sucrose. They were also able to modify at least two kinds of linear dextrans (1500 and 6000 $g.mol^{-1}$), making DSR-F-ΔSP-ΔGBD-CBM2a and DSR-F-ΔSP-ΔGBD biocatalysts to act as efficient α-transglucosidases in the presence of sucrose and linear oligodextrans. The additional cellulose-binding domain does not affect the modification capacity on linear oligodextrans of the fusion enzyme. These findings give new insights into the versatile reactions catalyzed by dextransucrases. Investigation of the relationship between structure and function of DSR-F variants will undoubtedly improve understanding of the polymerization mechanism of this enzyme and of GH70 glucansucrases in general. Considering its specificity, this fusion variant hold a great potential for the production of novel functional foods.

Author Contributions: Conceptualization, R.F. and R.A.; methodology, L.M.; software, R.F., E.D.; validation, M.L., A.M. and A.R.; formal analysis, R.F.; investigation, R.F., M.L., A.M. and A.R; resources, E.D.; data curation, R.F.; writing—original draft preparation, R.F.; writing—review and editing, R.F.; supervision, E.D.; project administration, B.M.; funding acquisition, B.M. All authors have read and agreed to the published version of the manuscript.

Funding: Please add: This research and the ACP were funded by Development Research Project financed by the Development Cooperation Program of ARES (Académie de Recherche et d'Enseigment Supérieur) from Belgium (2017-2022).

Acknowledgments: Reinaldo Fraga Vidal and Roberto C. Aríticas Ribalta were supported by a Development Research Project financed by the Development Cooperation Program of ARES (Académie de Recherche et d'Enseigment Supérieur) from Belgium (2017-2022). Reinaldo Fraga Vidal thanks William David Rau (MS Rau Antiques, New Orleans, USA) for his kind support. We thank Magali Remaud-Simeon and Pierre Monsan for their technical support. We also thank Dr. Joan Combie for the style correction of the manuscript.

Conflicts of Interest: The authors declare no conflict of interest. The funders had no role in the design of the study; in the collection, analyses, or interpretation of data; in the writing of the manuscript, or in the decision to publish the results.

References

1. Pu Y.; Zou Q.; Hou D., Zhang Y. and Chen S. Molecular weight kinetics and chain scission models for dextran polymers during ultrasonic degradation. *Carbohydr. Polym*. **2017**, *156*, 71–76. https://doi.org/10.1016/j.carbpol.2016.09.017
2. Zannini E.; Waters D.M.; Coffey A.; Arendt E.K. Production, properties, and industrial food application of lactic acid bacteria-derived exopolysaccharides. *Appl. Microbiol. Biotechnol*. **2016**, *100*, 1121–1135. http://doi.org./10.1007/s00253-015-7172-2
3. Vettori M.H.P.B.; Blanco K.C.; Cortezi M.; De Lima C.J.B. and Contiero J. Dextran: effect of process parameters on production, purification and molecular weight and recent applications. *Diálogos Cienc*. **2012**, 171–186. http://doi.org./10.7447/dc2012.018
4. Ryan P.M.; Ross R.P.; Fitzgerald G.F.; Caplice N.M.; Stanton C. Sugar-coated: exopolysaccharide producing lactic acid bacteria for food and human health applications. *Food Funct*. **2015**, 6 (3):679-93. http://doi.org./10.1039/c4fo00529e
5. Salazar N.; Gueimonde M.; De Los Reyes-Gavilán C.G.; Ruas-Madiedo P. Exopolysaccharides Produced by Lactic Acid Bacteria and Bifidobacteria as Fermentable Substrates by the Intestinal Microbiota. *Crit. Rev. Food Sci. Nutr*. **2016**, 56 (9):1440-53. https://doi.org/10.1080/10408398.2013.770728
6. Xu L. and Zhang J. Bacterial glucans: production, properties, and applications. *Appl. Microbiol. Biotechnol*. **2016**, 100 (21):9023-9036. https://doi.org/10.1007/s00253-016-7836-6
7. Naessens M.; Cerdobbek A.; Soetaert W.; Vandamme E.J. *Leuconostoc* dextransucrase and dextran: production, properties and applications. *J. Chem. Technol. Biotechnol*. **2005**, 80:845-860. https://doi.org/10.1002/jctb.1322
8. Semor N.; Azmi W.; Gautan M. Characterization and structural analysis of unique dextran synthesized by purified dextransucrase of newly isolated *Acetobacter tropicalis*. *Curr. Biotechnol*. **2018**, 7:376-386. https://doi.org/10.2174/2211550107666180905100531
9. Badel S.; Bernardi T.; Michaud P. New perspectives for Lactobacilli exopolysaccharides. *Biotechnol. Adv*. **2011**, 29 (1):54–66. https://doi.org/10.1016/j.biotechadv.2010.08.011
10. Zdolsek H.J.; Vegfors M.; Lindahl T.L.; Tornquist T.; Bortnik P. & Hahn R.G. Hydroxyethyl starches and dextran during hip replacement surgery: effects on blood volume and coagulation. *Acta Anaesthesiol. Scand*. **2011**, 55 (6):677-685. https://doi.org/10.1111/j.1399-6576.2011.02434.x

11. Monchois V.; Remaud-Simeon M.; Russel R.R.; Monsan P.; Willemot R.M. Characterization of *Leuconostoc mesenteroides* NRRL B-512F dextransucrase (DSRS) and identification of amino-acid residues playing a key role in enzyme activity. *Appl. Microbiol. Biotechnol.* **1997**, 48 (4):465-72. https://doi.org/10.1007/s002530051081
12. Lombard V.; Golaconda Ramulu H.; Drula E.; Coutinho P.M.; Henrissat B. The Carbohydrate-active enzymes database (CAZy) in 2013. *Nucl. Acids Res.* **2014**, 42:D490-D495. https://doi.org/10.1093/nar/gkt1178
13. Passerini D.; Vuillemin M.l.; Ufarté L.; Morel S.; Loux V.; Fontagné-Faucher C.; Monsan P.; Remaud-Siméon M.; Moulis C. Inventory of the GH70 enzymes encoded by *Leuconostoc citreum* NRRL B-1299–identification of three novel-transglucosylases. *FEBS J.* **2015**, 282 (11):2115-2130. https://doi.org/10.1111/febs.13261
14. Gangoiti J.; van Leeuwen S.; Gerwig G.; Duboux S.; Vafiadi C.; Pijning T.; Dijkhuizen L. 4,3-α-Glucanotransferase, a novel reaction specificity in glycoside hydrolase family 70 and clan GH-H. *Sci. Rep.* **2017**, 7, 39761; https://doi.org/10.1038/srep39761
15. Macgregor E.A.; Jespersen H.M.; Svensson B. A circularly permuted alpha-amylase-type alpha/beta-barrel structure in glucan-synthesizing glucosyltransferases. *FEBS Lett.* **1996**, 378:263-266. https://doi.org/10.1016/0014-5793(95)01428-4
16. Vujicić-Zagar A. and Dijkstra B.W. Monoclinic crystal form of *Aspergillus niger* alpha-amylase in complex with maltose at 1.8 angstroms resolution. *Acta Crystallogr. Sect. F Struct. Biol. Cryst, Commun*. **2006**, 62(Pt8):716-21. https://doi.org/10.1107/s1744309106024729
17. Pijning T.; Vujicic-Zagar A.; Kralj S.; Eeuwema W.; Dijkhuizen L.; Dijkstra, B.W. Biochemical and crystallographic characterization of a glucansucrase from *Lactobacillus reuteri* 180. *Biocat. Biotrans.* **2008**, 26(1-2):12-17. https://doi.org/10.1080/10242420701789163
18. Molina M.; Cioci G.; Moulis C.; Séverac E.; Remaud-Simeon M. Bacterial α-Glucan and branching sucrases from GH70 Family: Discovery, structure-function relationship studies and engineering. *Microorganisms* **2021**, 9:1607. https://doi.org/10.3390/microorganisms9081607
19. Fraga R.; Moulis C.; Escalier P.; Remaud-Simeón M.; Monsan P. Isolation of a Gene from *Leuconostoc citreum* B/110-1-2 Encoding a Novel Dextransucrase Enzyme. *Curr. Microbiol.* **2011**, 62:1260-1266. https://doi.org/10.1007/s00284-010-9851-7
20. Fraga R.; Martínez A.; Moulis C.; Escalier P.; Morel S.; Remaud-Siméon M.; Monsan P. A novel dextransucrase is produced by *Leuconostoc citreum* strain B/110-1-2: an isolate used for the industrial production of dextran and dextran-derivatives. *J. Ind. Microbiol. Biotechnol.* **2011**, 38:1499-1503. https://doi.org/10.1007/s10295-010-0936-x
21. Fraga R.; Pacios S.; Arísticas R.C.; Martínez L.; Lafargue M.; Montes A.; Remaud-Simeon M.; Monsan P. Cloning and Partial Characterization of an Extracellular Dextransucrase Coding Region (DSR-V) from *Leuconostoc citreum* M-3. In: *Microbial Exopolysaccharides: Current Research and Developments*. Chapter 11, 1st ed.; Ed. Özlem Ateş Duru; Caister Academic Press, Norfolk, UK, 2019; pp. 295-314. https://doi.org/10.21775/9781912530267 https://doi.org/10.21775/9781912530267.11
22. Joucla G.; Pizzut S.; Monsan P.; Remaud-Simeon M. Construction of a fully active truncated alternansucrase partially deleted of its carboxy-terminal domain. *FEBS Lett.* **2006**, 580:763-768. https://doi.org/10.1016/j.febslet.2006.01.001
23. Olivares-Illana V.; López-Munguía A.; Olvera C. Molecular characterization of inulosucrase from *Leuconostoc citreum*: a fructosyltransferase within a glucosyltransferase. *J. Bacteriol.* **2003**, 185:3606-3612. https://dx.doi.org/10.1128%2FJB.185.12.3606-3612.2003
24. Vuillemin M.; Claverie M.; Brison Y.; Séverac E.; Bondy P.; Morel S.; Monsan P.; Moulis, C.; and Remaud-Siméon M. Characterization of the first α-(1→3) branching sucrases of the GH70 family. *J. Biol. Chem.* **2016**, 291:7687-7702. https://doi.org/10.1074/jbc.m115.688044
25. Parlak M.; Ustek D.; Tanriseven A. Designing of a novel dextransucrase efficient in acceptor reactions. *Carbohydr. Res.* **2014**, 386:41-47. https://doi.org/10.1016/j.carres.2014.01.003
26. Hong J.; Wang Y.; Ye X.; Percival Zhang Y.H. Simple protein purification through affinity adsorption on regenerated amorphous cellulose followed by intein self-cleavage. *J. Chromatogr. A* **2008**, 1194:150-154. https://doi.org/10.1016/j.chroma.2008.04.048
27. Meng X.; Dobruchowska J.M.; Pijning T.; Gerwig G.J.; Kamerling J.P.; Dijkhuizen L. Truncation of domain V of the multidomain glucansucrase GTF180 of *Lactobacillus reuteri* 180 heavily impairs its polysaccharide-synthesizing ability. *Appl. Microbiol. Biotechnol.* **2015**, 99:5885-5894. https://doi.org/10.1007/s00253-014-6361-8
28. Molina M.; Moulis C.; Monties N.; Pizzut-Serin S.; Guieysse D.; Morel S.; Cioci G.; Remaud-Simeon M. Deciphering an undecided enzyme: Investigations of the structural determinants involved in the linkage specificity of alternansucrase. *ACS Catal*. **2019**, 9 (3):2222-2237. https://doi.org/10.1021/acscatal.8b04510
29. Moulis C.; Joucla G.; Harrison D.; Fabre E.; Potocki-Veronese G.; Monsan P.; Remaud-Simeon M. Understanding the polymerization mechanism of glycoside-hydrolase family 70 glucansucrases. *J. Biol. Chem.* **2006**, 281:31254-31267. https://doi.org/10.1074/jbc.m604850200
30. Tsuchiya H.M.; Hellman N.N.; Koepsell H.J. Factors affecting the molecular weight of enzymatically synthesized dextran. *J. Am. Chem. Soc.* **1953**, 75 (3):757–758. https://doi.org/10.1021/ja01099a521
31. Bechtner J.; Hassler V.; Wefers D.; Vogel R.F.; Jakob F. Insights into extracellular dextran formation by Liquorilactobacillus nagelii TMW 1.1827 using secretomes obtained in the presence or absence of sucrose. *Enzyme Microb. Technol.* **2021**, 143:109724. https://doi.org/10.1016/j.enzmictec.2020.109724
32. Binder T.P.; Cote G.L.; Robyt G.F. Disproportionation reactions catalyzed by *Leuconostoc* and *Streptococcus* glucansucrases. *Carbohydr. Res.* 1983, 124 (2): 275-286. https://doi.org/10.1016/0008-6215(83)88463-8

Preprints (www.preprints.org) | NOT PEER-REVIEWED | Posted: 1 September 2021 doi:10.20944/preprints202109.0013.v1

33. López-Munguía A.; Pelenc V.; Remaud-Simeon M.; Biton J.; Michel J.M.; Lang C.; Paul F.; Monsan P. Production and purification of alternansucrase, a glucosyltransferase from *Leuconostoc mesenteroides* NRRL B-1355, for the synthesis of oligoalternans. *Enzyme Microb. Technol.* **1993**, 15 (1):77-85.
34. Ozimek, L.K.; Krajl S.; van der Maarel M.J.E.C.; Dijkhuizen L. The levansucrase and inulosucrase enzymes of *Lactobacillus reuteri* 121 catalyse processive and non-processive transglycosylation reactions. *Microbiology* **2006**, 152 (4):1187-1196. https://doi.org/10.1099/mic.0.28484-0
35. Molina M.; Moulis C.; Monties N.; David G.; Morel S.; Cioci G.; Remaud-Simeon M. A specific oligosaccharide-binding site in the alternansucrase catalytic domain mediates alternan elongation. *J. Biol. Chem.* **2020**, 295:9474-9489. https://doi.org/10.1074/jbc.ra120.013028
36. Zhang Y-H. P.; Cui J.; Lynd L.R.; Kuang L.R. A transition from cellulose swelling to cellulose dissolution by *o*-phosphoric acid: evidence from enzymatic hydrolysis and supramolecular structure. *Biomacromolecules* **2006**, 7(2):644-648. https://doi.org/10.1021/bm050799c
37. Sumner J.; Howell S. A method for determination of invertase activity. *J. Biol. Chem.* **1935**, 108:51-54.
38. Bradford M.M. A rapid and sensitive method for the quantitation of microgram quantities of protein utilizing the principle of protein-dye binding. *Anal. Biochem.* **1976**, 72: 248-254. https://doi.org/10.1016/0003-2697(76)90527-3
39. Miller A.W.; Robyt J.F. Detection of dextransucrase and levansucrase on polyacrylamide gels by the periodic acid-Schiff stain: staining artifacts and their prevention. *Anal. Biochem.* **1986**, 156:357-363. https://doi.org/10.1016/0003-2697(86)90266-6
40. Fernandez-Patrón C.; Hardy E.; Seoane J.; Castellanos L. Double staining of coomassie blue-stained polyacrylamide gels by imidazole-sodium dodecyl sulfate-zinc reverse staining: sensitive detection of coomassie blue-undetected proteins. *Anal. Biochem.* **1995**, 224 (1):263-269. https://doi.org/10.1006/abio.1995.1039